Chapter 10 summary
Theory of activation barriers

Key concept: Barriers to reaction are caused by

Table 10.1 Principle causes of barriers to chemical reactions.
• Bond Stretching and Distortion • Orbital Distortion due to Pauli Repulsions • Quantum Effects • Special Reactivity of Excited States

Model I (Polayni's model): Assume Barriers caused by bond stretching

Consider a proton transfer reaction

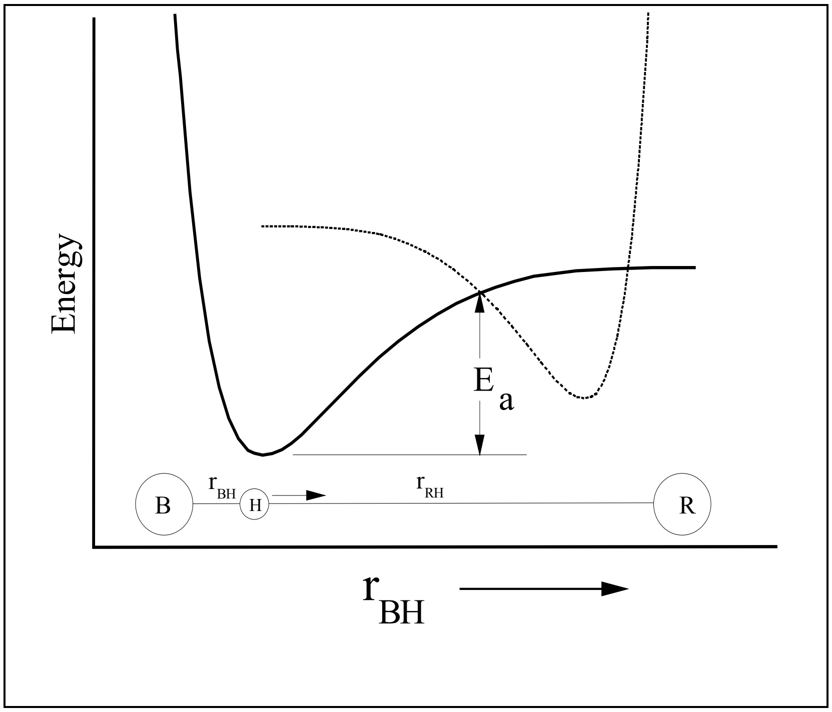

Figure 10.2 The energy changes which occur when a proton H is transferred between a conjugate base B and a reactant R. The solid line is the energy of the B-H bond while the dotted line is the energy of the H-R bond.

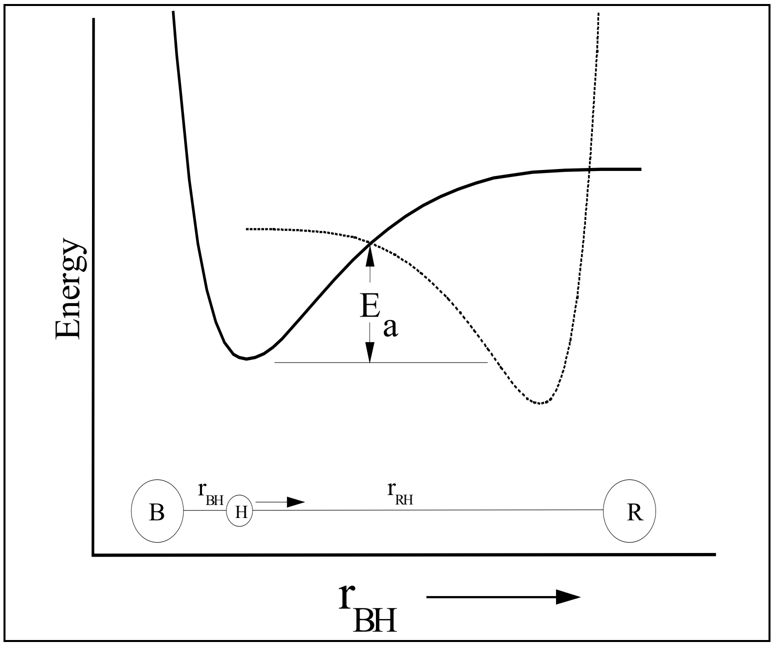

Figure 10.3 A diagram illustrating how an upward displacement of the B-H curve affects the activation energy when the B-R distance is fixed.

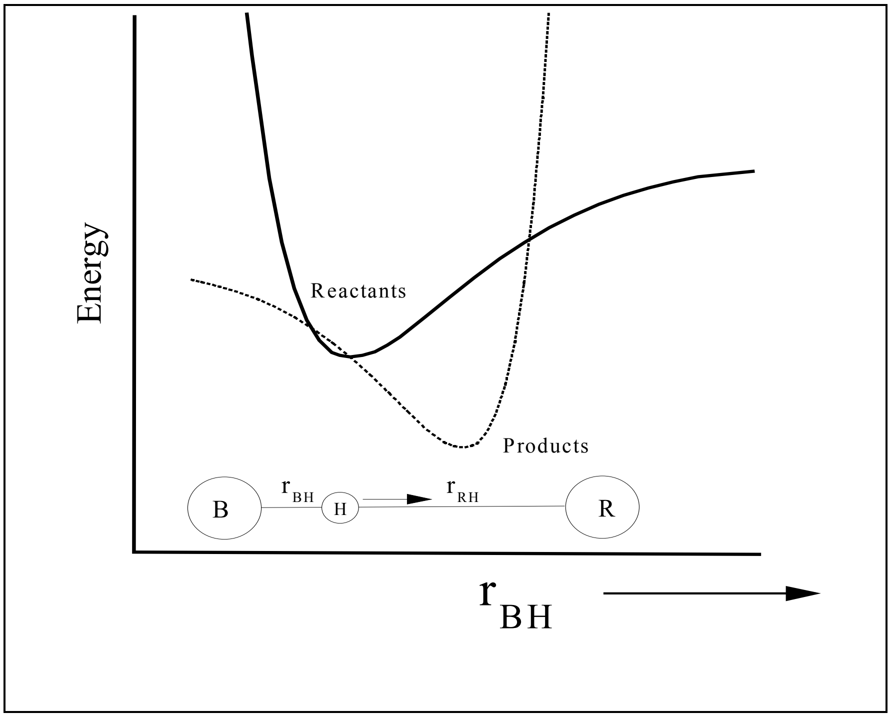

Figure 10.4 A diagram illustrating a case where the activation energy is zero.

Derivation of the Polayni equation

Key approximations

- Barriers caused by bond stretching
- Linearize potential as shown in 10.9
- Associate barrier with curve crossing

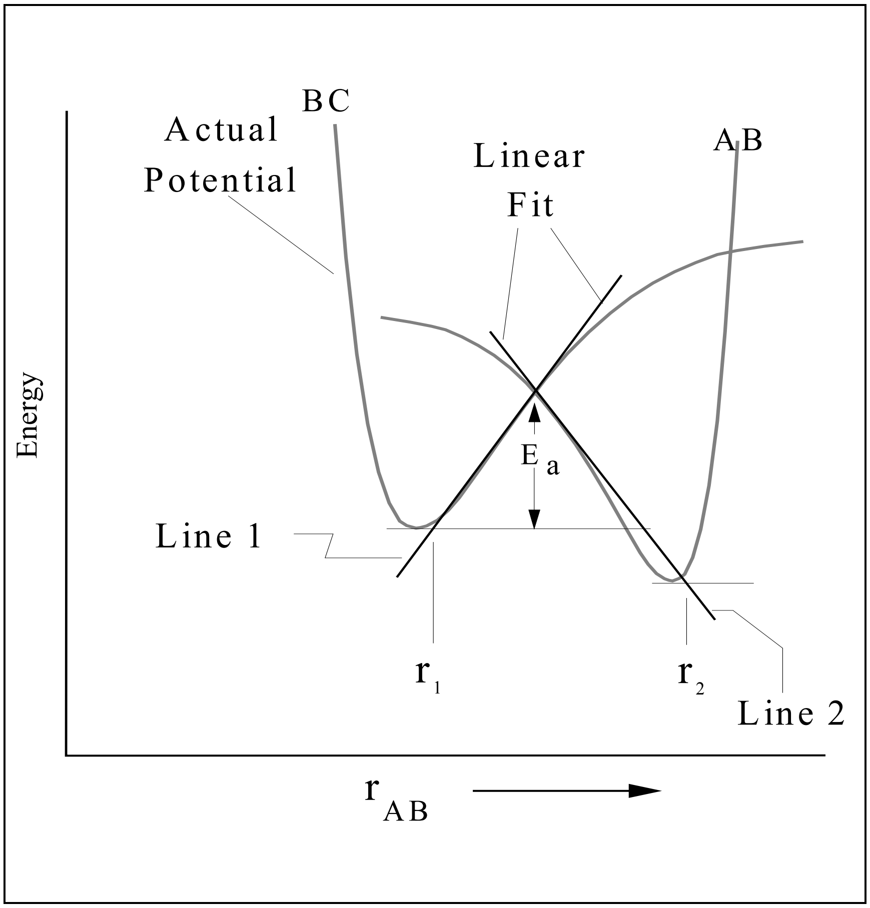

Figure 10.6 A linear approximation to the Polanyi diagram used to derive equation (10.11).

$$E_1 = E_{\mathrm{Reactant}} + |Sl_1|(r_{ABC} - r_1) \qquad \text{(reactants)}$$

(10.9)

$$E_2 = E_{\mathrm{product}} + |Sl_2|(r_2 - r_{ABC}) \qquad \text{(products)}$$

(10.10)

setting the two lines equal yields

$$E_a = \left(\frac{|Sl_1||Sl_2|}{|Sl_1| + |Sl_2|}\right)(r_2 - r_1) + \frac{|Sl_1|}{|Sl_1| + |Sl_2|}\Delta H_r$$

(10.11)

defining

$$E_a^o = \left(\frac{|Sl_1||Sl_2|}{|Sl_1| + |Sl_2|}\right)(r_2 - r_1)$$

(10.12)

$$\gamma_P = \frac{|Sl_1|}{|Sl_1| + |Sl_2|}$$

(10.13)

yields

$$\boxed{E_a = E_a^o + \gamma_P \Delta H_r}$$

(10.14)

Predicts bond energy varies linearly with heat of reaction.

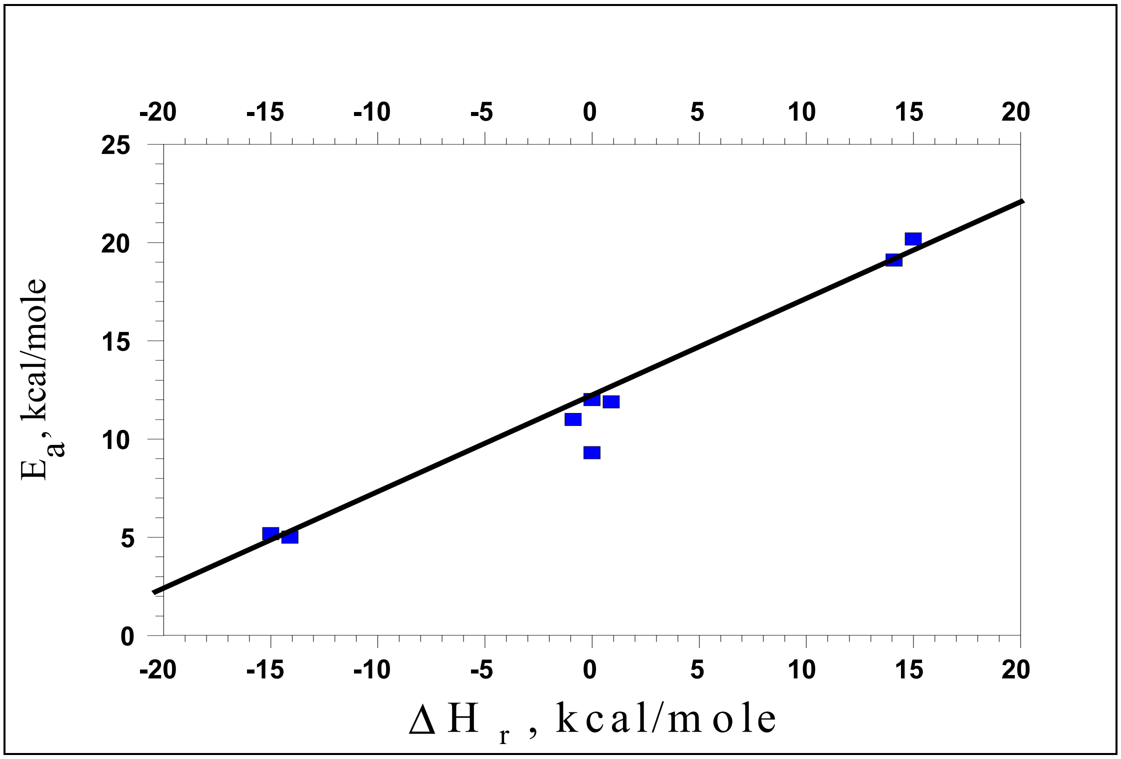

Figure 10.7 A plot of the activation barriers for the reaction R + H R′ → RH + R′ with R, R = H, CH_3, OH plotted as a function of the heat of reaction ΔH_r.

Data shows approximate linear behavior over limited range of potential

Not a good approximation over a wide range of potential:

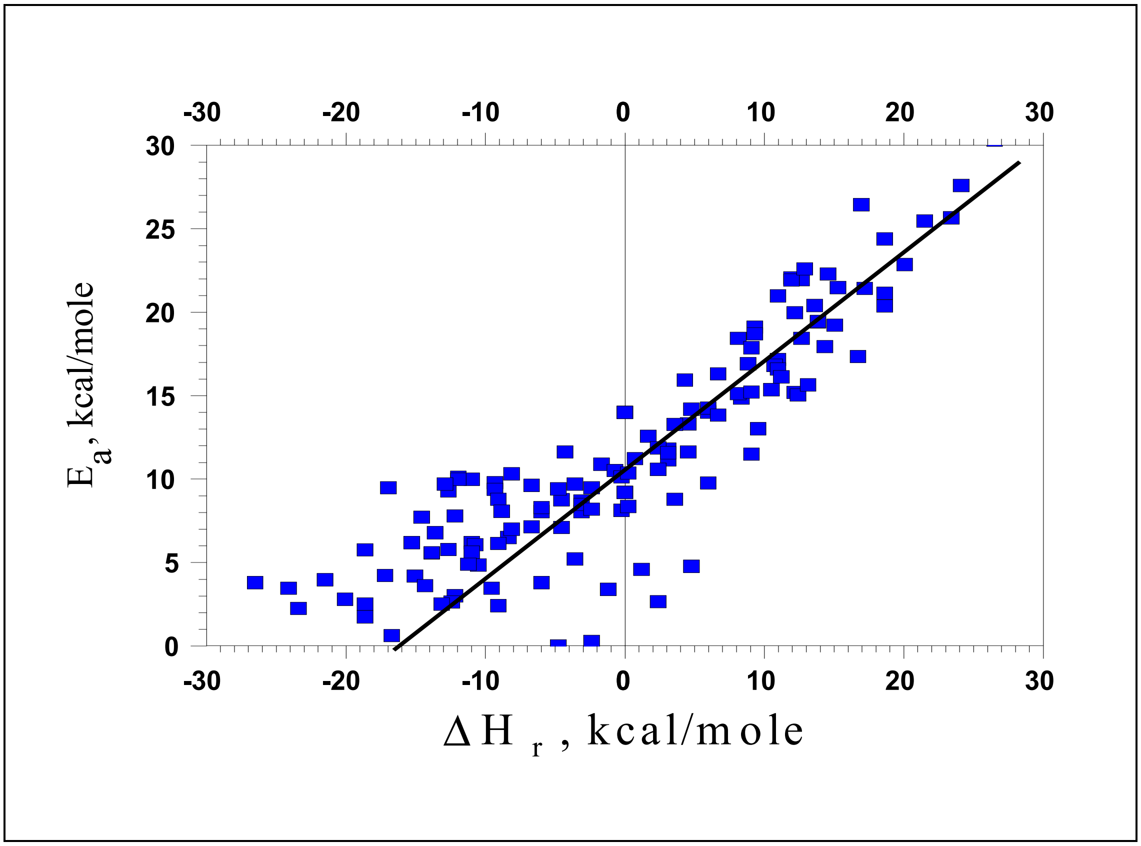

Figure 10.10 A Polanyi relationship for a series of reactions of the form RH + R′ → R + HR′. Data from Roberts and Steel[1994].

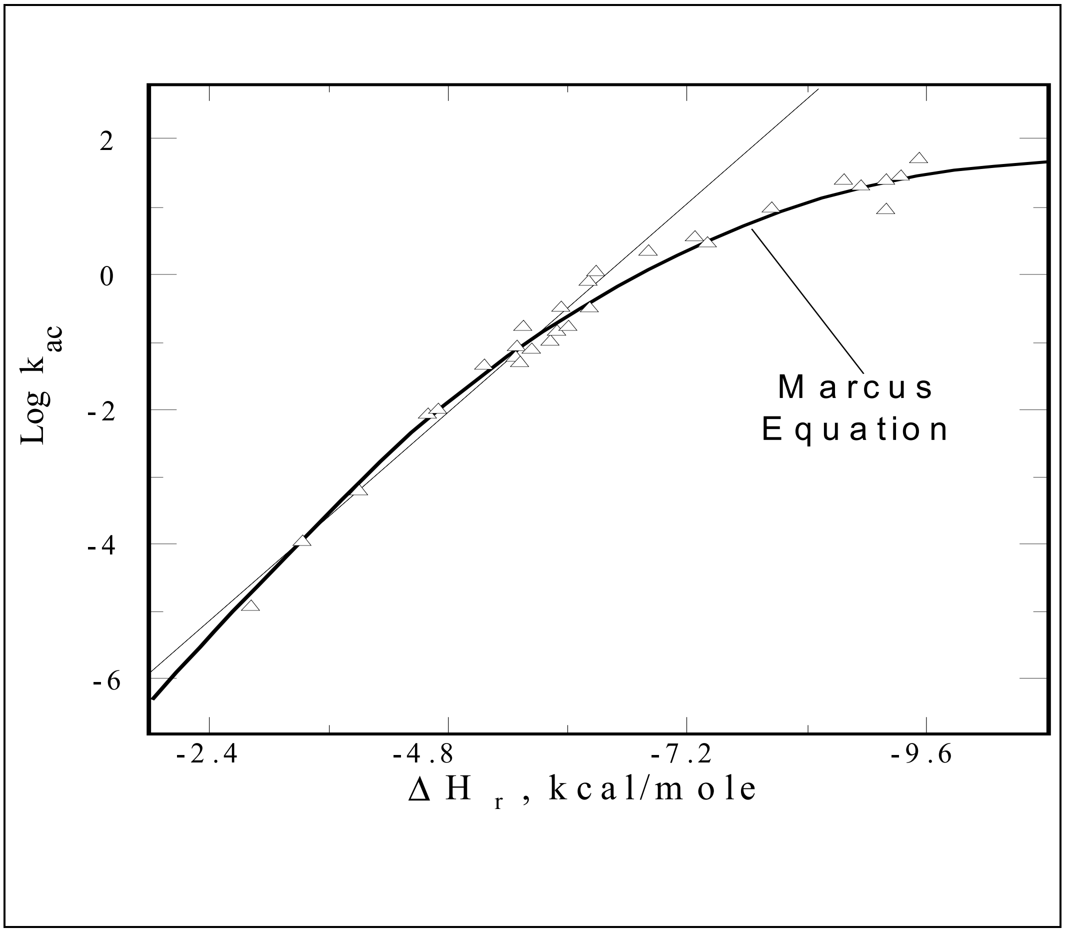

Figure 10.11 A Polanyi plot for the enolization of $NO_2(C_6H_4)O(CH_2)_2COCH_3$. Data of Hupke and Wu[1977]. Note Ln (k_{ac}) is proportional to E_a.

Key prediction of model: bonds that are weak (i.e. easier to stretch) are easier to break than strong bonds.

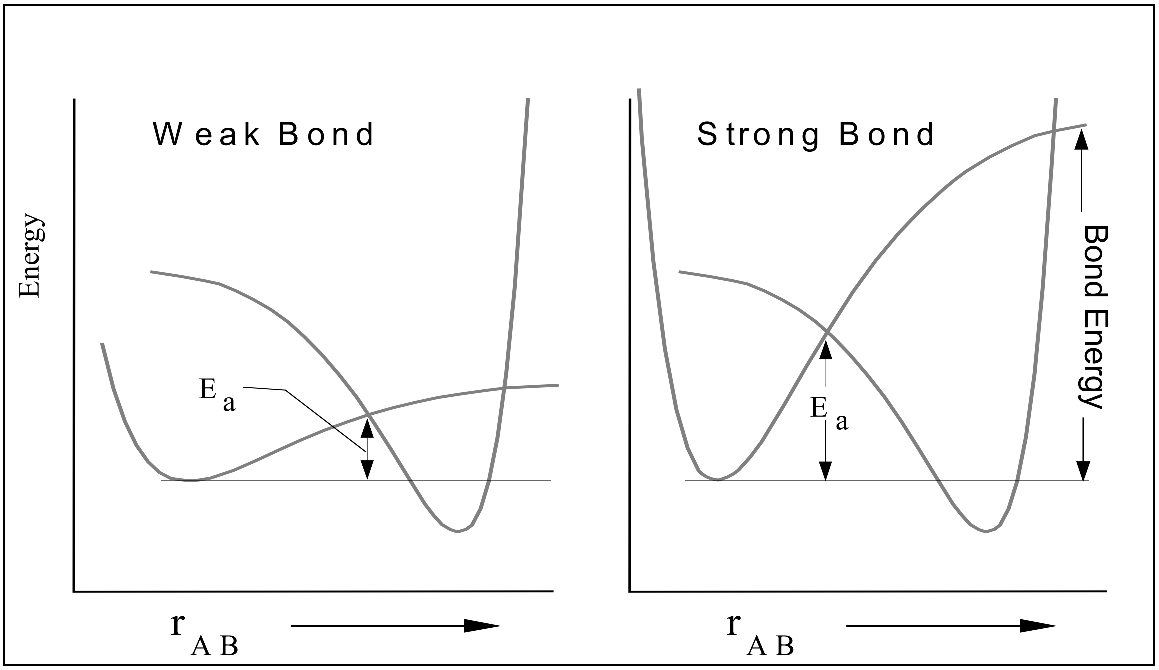

Figure 10.8 A schematic of the curve crossing during the destruction of a weak bond and a strong one for the reaction AB + C → A + BC.

Experiment ***does not*** confirm predicted trend

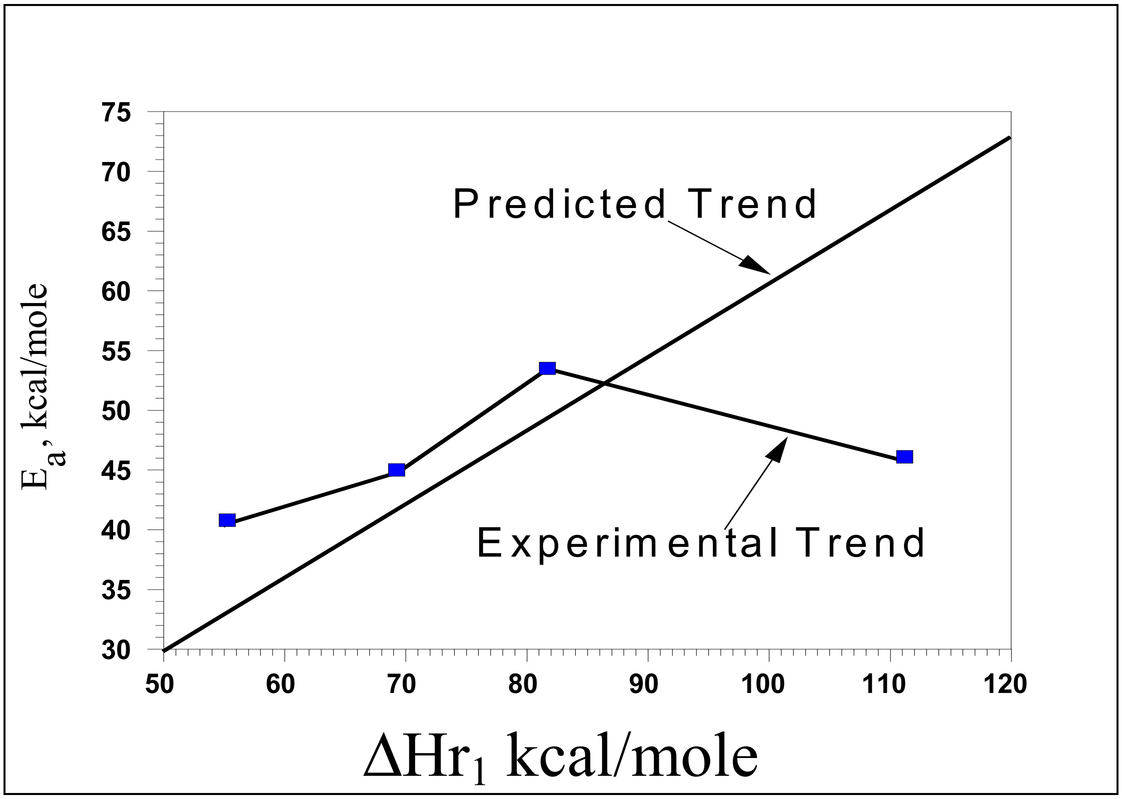

Figure 10.9 The activation barrier for the reaction $X^- + CH_3X \rightarrow XCH_3 + X^-$. The numbers are from the calculations of Glukhoustev, Pross and Radam[1995].

Still people use the method when nothing else is available.

Table 5.4 Intrinsic barriers and transfer. Coefficients for different types of reaction of neutral species.

Reaction	Example	Actual E_A^o kcal/mole	E_A^o to assume when predicting mechanisms kcal/mole	Actual γ_P	γ_P to assume when predicting mechanisms
Simple bond scission	$AB+X \rightarrow A+B+X$ X=a collision partner	0-1	1	1.0	1.0
Recombination	$A+B+X \rightarrow AB+X$ X=a collision partner	0-1	1	1.0	1.0
Atom transfer reaction $0 > \Delta Hr > -40$	$R\,x + R^1 \rightarrow R + x\text{-}R^1$ x = an atom	8-16	12	0.2 to 0.6	0.3
Atom transfer reaction $0 \leq \Delta Hr \leq 40$	$R\text{-}\,x + R \rightarrow R + x\text{-}R^1$ x=an atom	8-16	12	0.4 to 0.8	0.7
Atom transfer reaction $\Delta Hr < -40$	$R\text{-}\,x + R \rightarrow R + x\text{-}R^1$ x=an atom	0-2	0	0	0
Atom transfer reaction $\Delta Hr > 40$	$R\text{-}\,x + R \rightarrow R + x\text{-}R^1$ x=an atom	0-5	2	0.9-1.0	1.0
Ligand transfer reaction to hydrogen	$H+R\text{-}R^1 \rightarrow HR + R^1$	40-50	45	0.4 to 0.6	0.5
Other ligand transfer reactions	$x + R\text{-}R^1 \rightarrow xR + R^1$ x=an atom	50 or more	50	0.3 to 0.7	0.5

Seminov approximation: assume linear over a limited range of ΔH

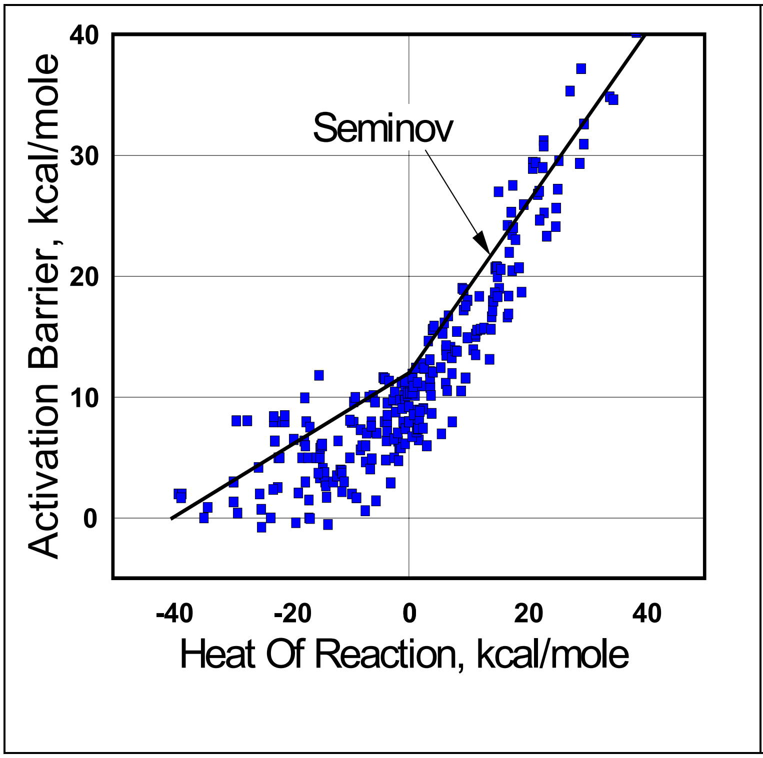

Figure 11.11 A comparison of the activation energies of a number of hydrogen transfer reactions to those predicted by the Seminov relationships, equations (11.33) and (11.34)

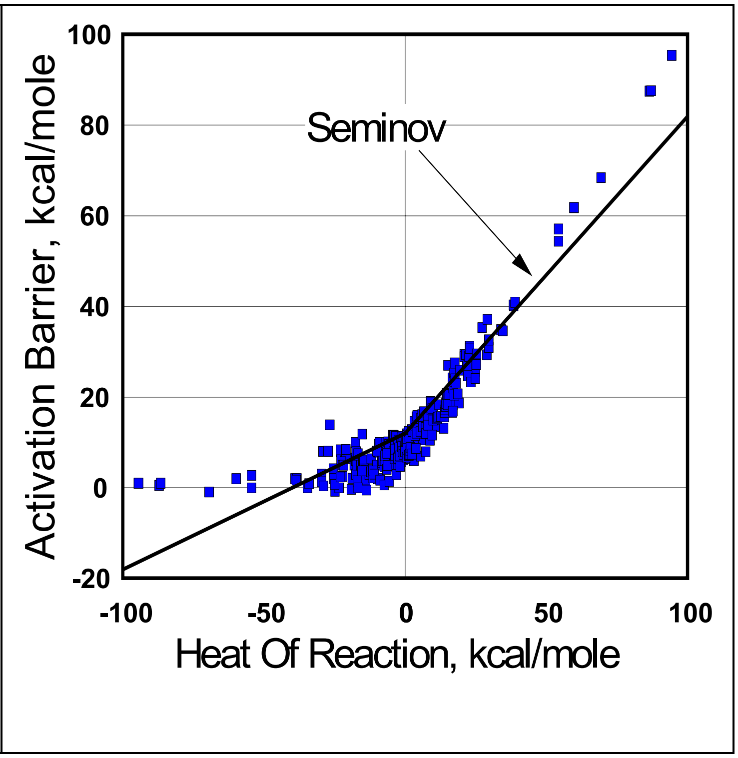

Figure 11.12 A comparison of the activation energies of 482 hydrogen transfer reactions to those predicted by the Seminov relationships, over a wider range of energies.

Only fair approximation. Still good enough to make useful predictions of mechanisms: see solved problem 5.A and 5.B

Fails because

a) linearization of potential in figure 10.6 not particular accurate

b) Pauli repulsions important to barriers

The Marcus equation. Assume

- Bond stretching controls barriers.
- Potential parabolic in position.

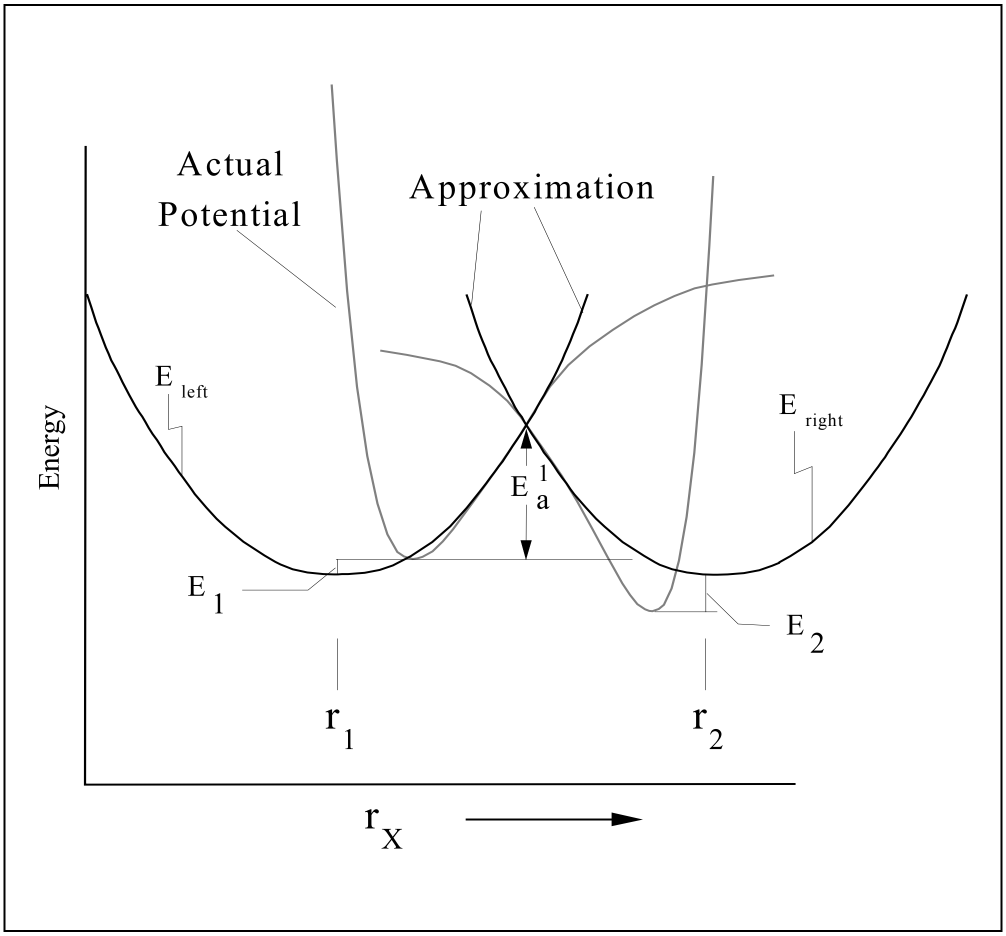

Figure 10.13 An approximation to the change in the potential energy surface which occurs when ΔH_r changes.

Explains curvature of Polayni Plots

$$E_{\mathrm{left}}(r_X) = SS_1(r_X - r_1)^2 + E_1$$
(10.21)

$$E_{\mathrm{right}}(r_X) = SS_2(r_X - r_2)^2 + \Delta H_r + E_2$$
(10.22)

solving

$$SS_1(r^{\ddagger} - r_1)^2 + E_1 = SS_2(r^{\ddagger} - r_2)^2 + E_2 + \Delta H_r$$
(10.23)

$$SS_1 = SS_2$$
(10.24)

Result

$$E_A = \left(1 + \frac{\Delta H_r}{4E_a^0}\right)^2 E_a^0 + w_r$$
(10.31)

$$\boxed{E_A = \left(1 + \frac{\Delta H_r}{4E_a^0}\right)^2 E_a^0}$$

(10.33)

Qualitative features of the Marcus equation

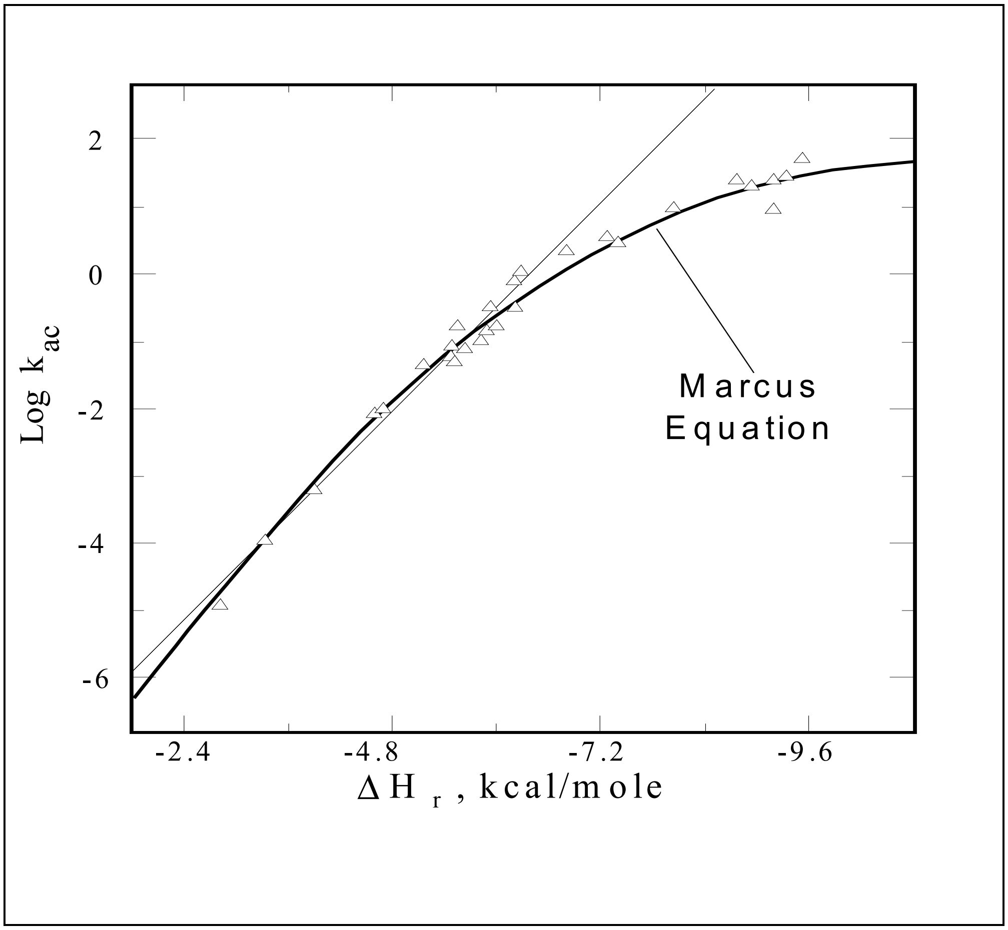

Figure 10.11 A Polanyi plot for the enolization of $NO_2(C_6H_4)O(CH_2)_2COCH_3$. Data of Hupke and Wu[1977]. Note Ln (k_{ac}) is proportional to E_a.

Marcus is great for unimolecular reactions

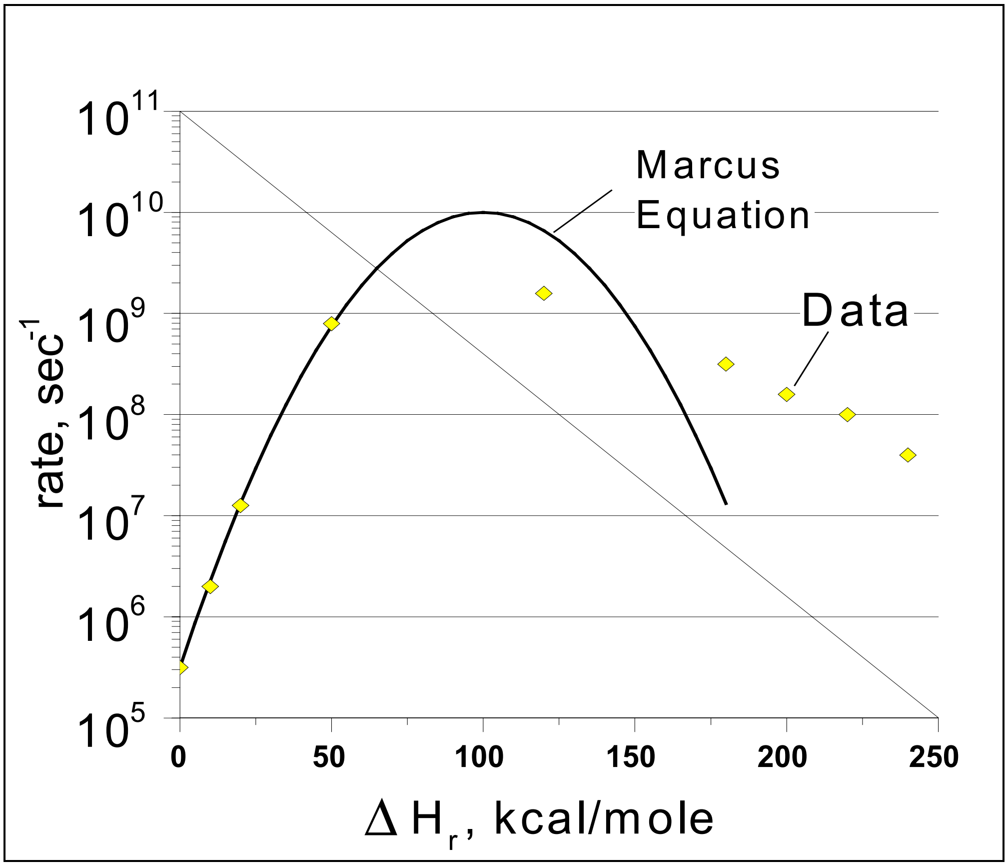

Figure 10.17 The activation energy for intramolecular electron transfer across a spacer molecule plotted as a function of the heat of reaction. Data of Miller et. al., J. Am. Chem. Soc., **106** (1984) 3047.

Not as good for Bimolecular reactions

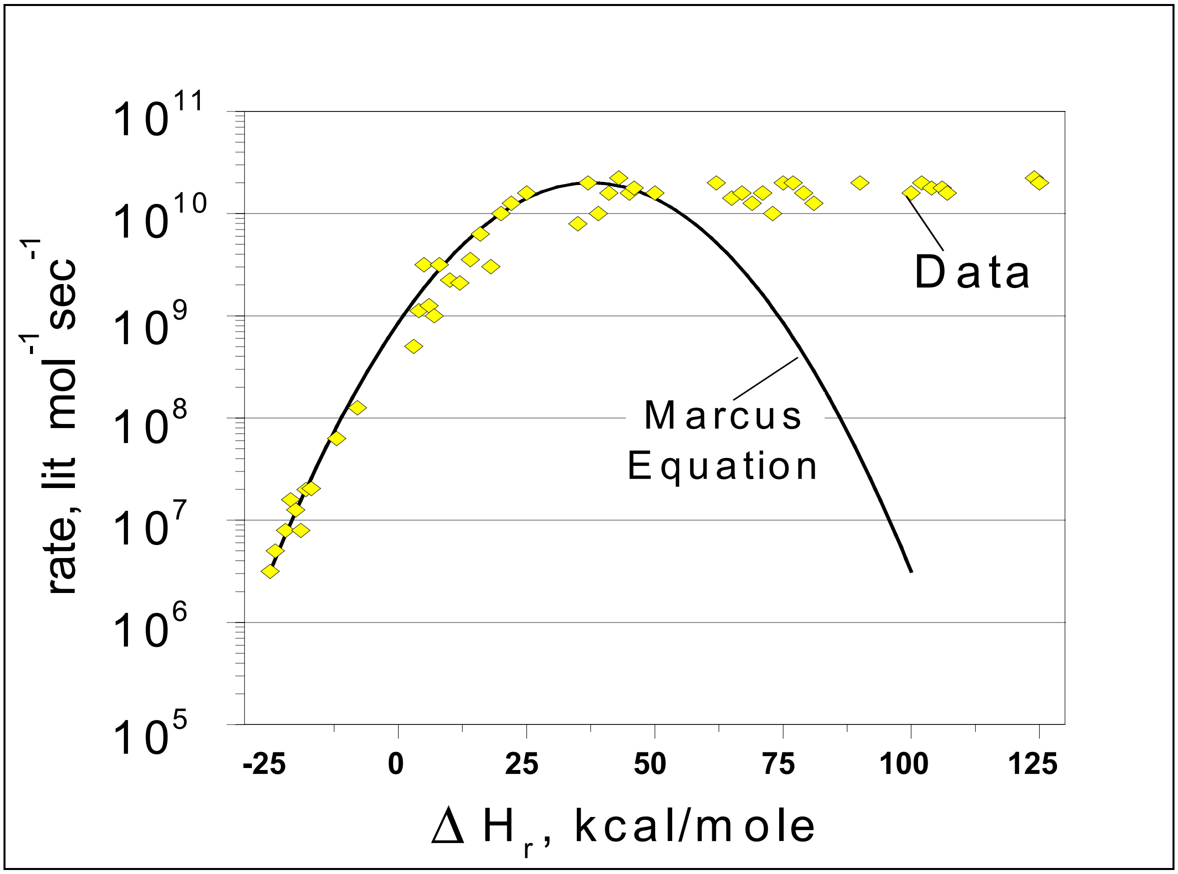

Figure 10.18 The activation energy for florescence quenching of a series of molecules in acetonitrite plotted as a function of the heat of reaction. Data of Rehm et. al., Israel J. Chem. **8** (1970) 259.

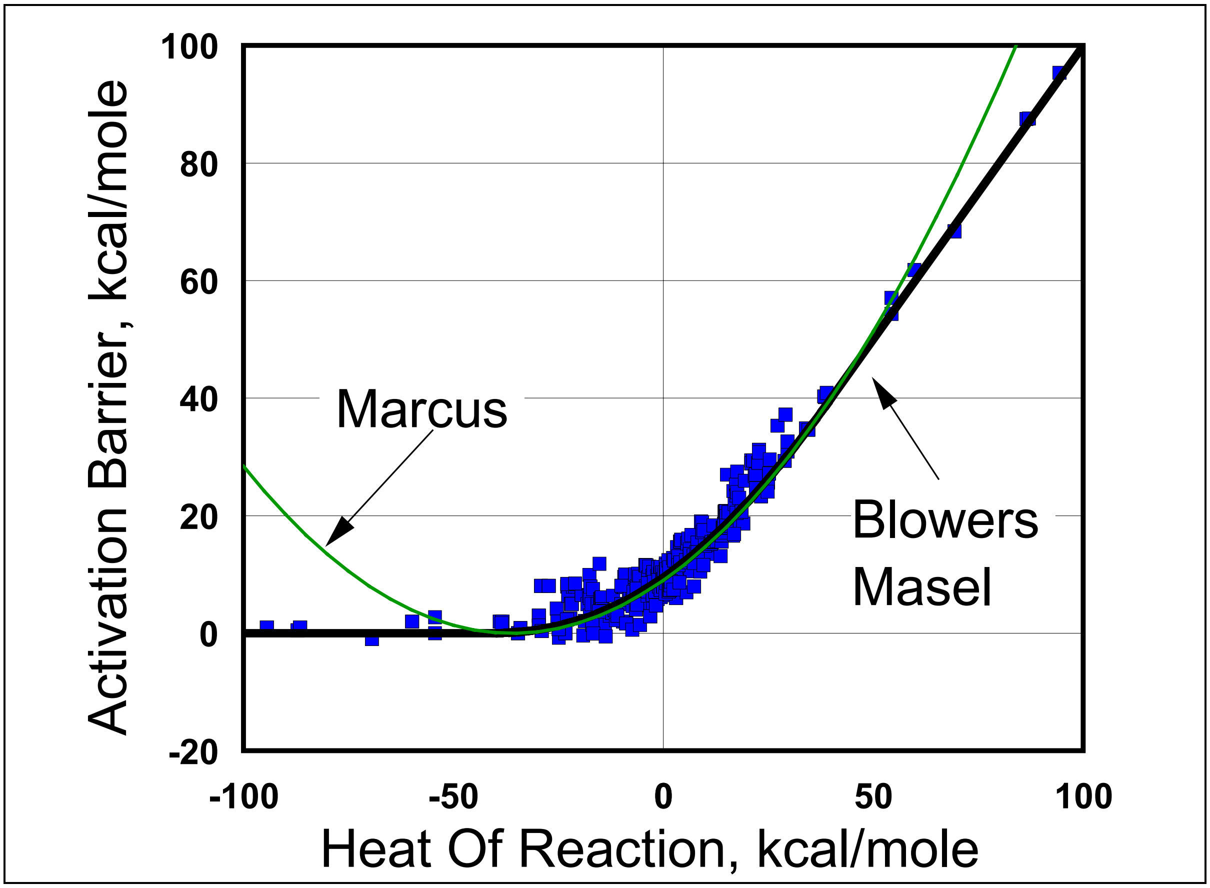

Figure 10.29 A comparison of the barriers computed from Blowers and Masel's model to barriers computed from the Marcus equation and to data for a series of reactions of the form $R + HR^1 \rightarrow RH + R^1$ with $w_O = 100$ kcal/mole and $E_A^O = 10$ kcal/mole.

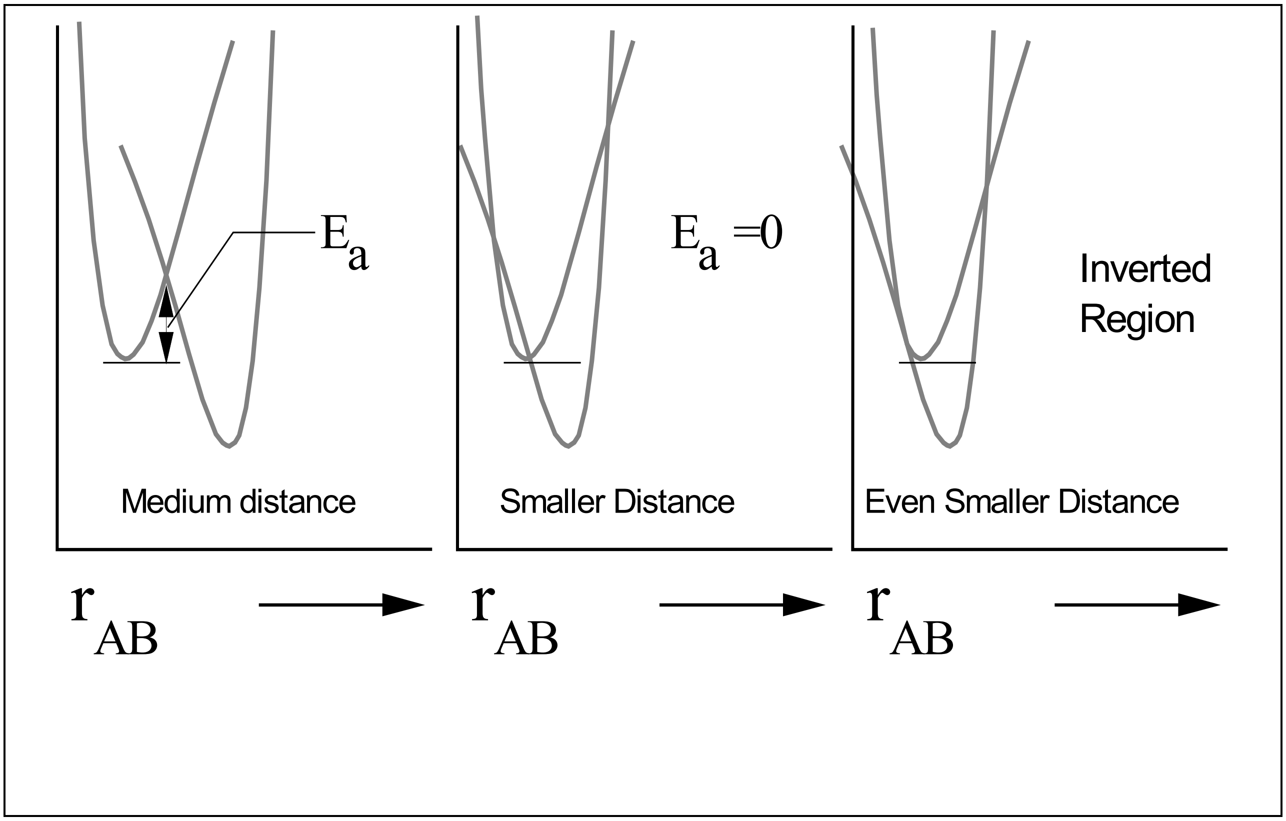

Figure 10.19 Changes in the curve crossing model as (r_2-r_1) decreases dorms the reaction $AB + C \rightarrow A + BC$.

Example 11.F Activation barriers via the Marcus approximation

Use the Marcus equation to estimate the activation barrier for the reaction

$H + CH_3CH_3 \rightarrow H_2 + CH_2CH_3$

Solution

According to table 11.3 E_A^0=10 kcal/mole.

choose ΔH_r=-2 kcal/mole from example 11.C

$$E_a = E_A^0\left(1+\frac{\Delta H}{4E_A^0}\right)^2 \tag{11.F.4}$$

From the data above E_A^0=10 kcal/mole, ΔH_r=-2 kcal/mole. Plugging into equation (11.F.4)

$$E_a = 10\text{kcal/mole}\left(1+\frac{-2\text{kcal/mole}}{4(10\text{kcal/mole})}\right)^2 = 9.0 \quad \text{kcal/mole}$$

By comparison the experimental value from Westley is 9.6 kcal/mole.

ChE 387
Lect 34
Theory of activation barriers

Key concept: Barriers to reaction are caused by

Table 10.1 Principle causes of barriers to chemical reactions.

- Bond Stretching and Distortion
- Orbital Distortion due to Pauli Repulsions
- Quantum Effects
- Special Reactivity of Excited States

So far, we have discussed

- Polayni relationship

$$\boxed{E_a = E_a^o + \gamma_P \Delta H_r}$$

(10.14)

- Marcus equation

$$\boxed{E_A = \left(1 + \frac{\Delta H_r}{4E_a^0}\right)^2 E_a^0}$$

(10.33)

Polayni works only over a limited range of ΔH

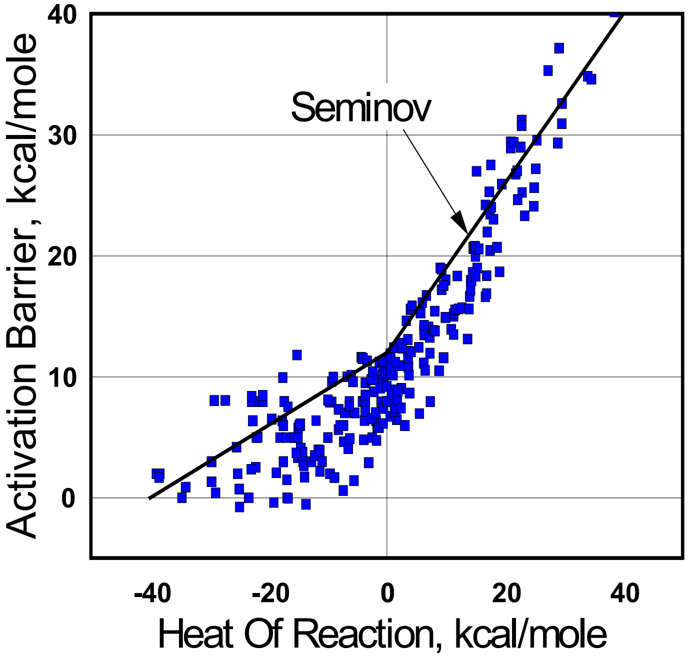

Figure 11.11 A comparison of the activation energies of a number of hydrogen transfer reactions to those predicted by the Seminov relationships, equations (11.33) and (11.34)

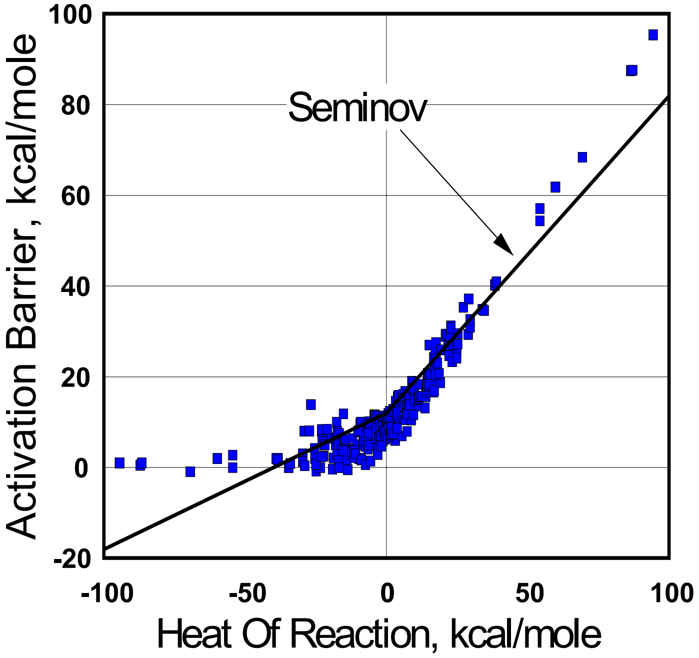

Figure 11.12 A comparison of the activation energies of 482 hydrogen transfer reactions to those predicted by the Seminov relationships, over a wider range of energies.

Marcus good for unimolecular reactions where geometry fixed

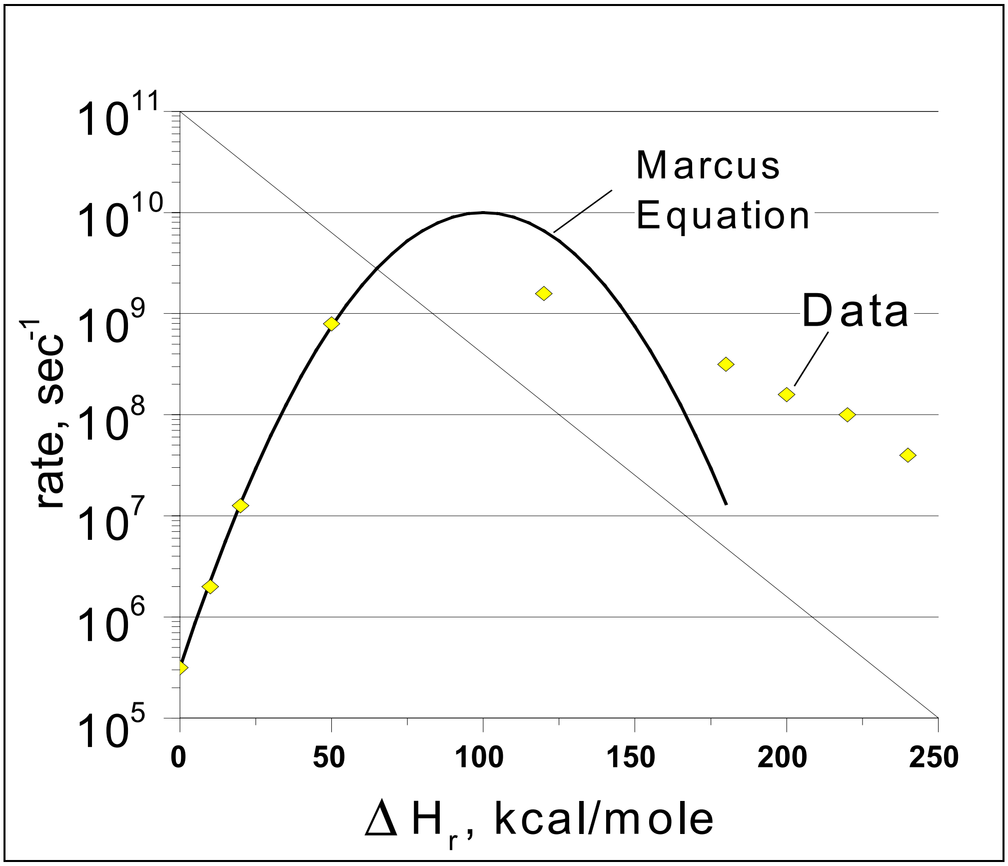

Figure 10.17 The activation energy for intramolecular electron transfer across a spacer molecule plotted as a function of the heat of reaction. Data of Miller et. al., J. Am. Chem. Soc., **106** (1984) 3047.

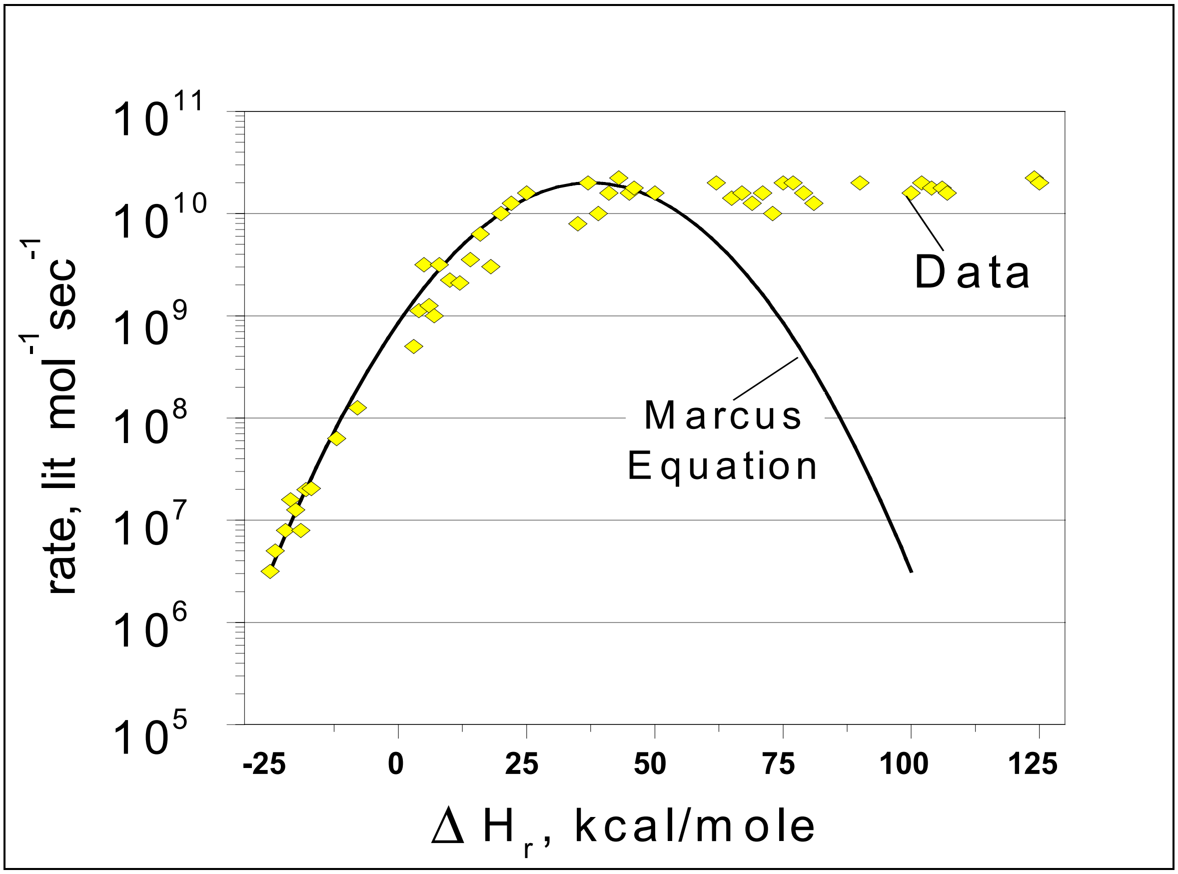

Figure 10.18 The activation energy for florescence quenching of a series of molecules in acetonitrite plotted as a function of the heat of reaction. Data of Rehm et. al., Israel J. Chem. **8** (1970) 259.

Not as good for Bimolecular reactants

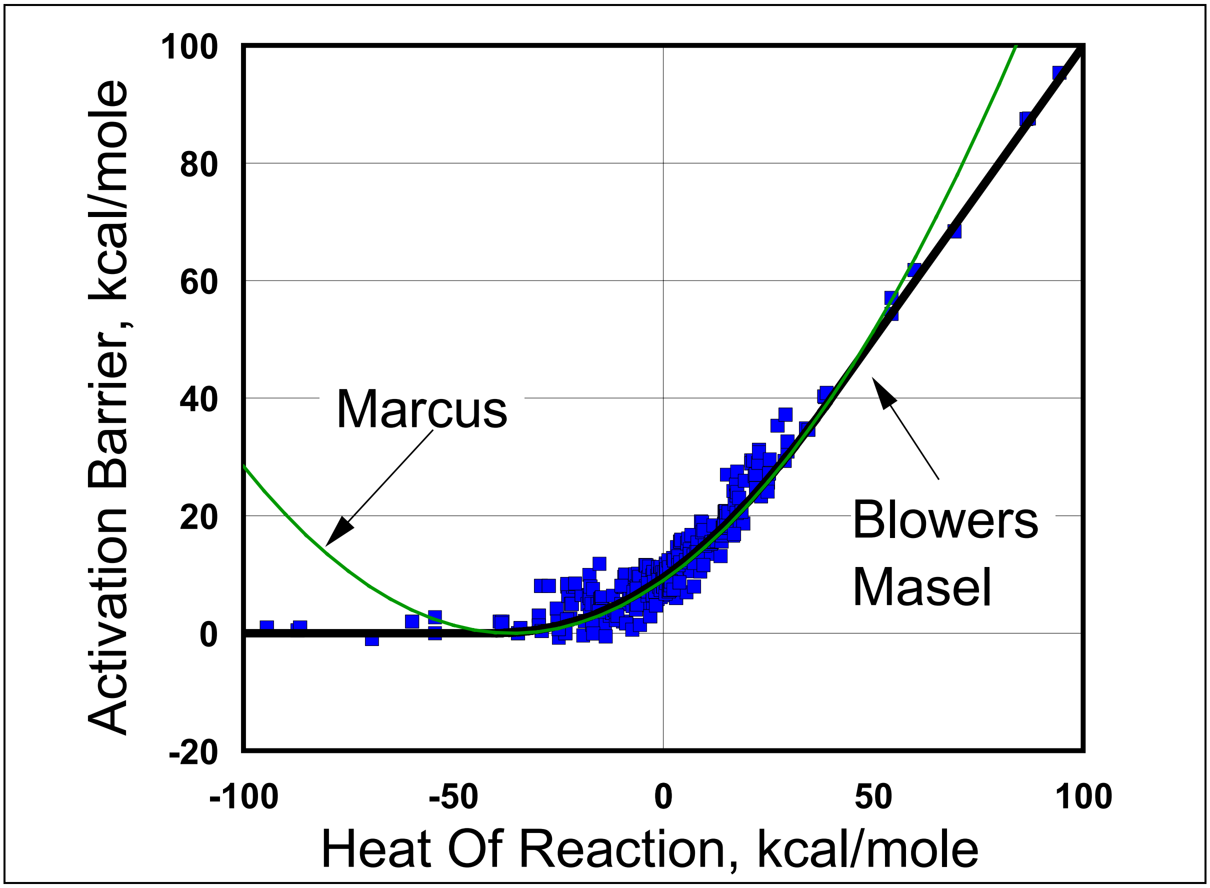

Figure 10.29 A comparison of the barriers computed from Blowers and Masel's model to barriers computed from the Marcus equation and to data for a series of reactions of the form $R + HR^1 \rightarrow RH + R^1$ with $w_O = 100$ kcal/mole and $E_A^O = 10$ kcal/mole.

Next Topic: Blowers-Masel Approximation

Newer Approx. (1999)

Derivation

$$V(\rho_{CC},\rho_{CH}) = E_{CC}(\rho_{CC}) + E_{CH}(\rho_{CH}) + V_{Pauli}$$
(10.52)

$$V(\rho_{CC},\rho_{CH}) = w_{CC}\left(\left[\exp\left(-\alpha_{CC}(\rho_{CC}-\rho_{CC}^{e})\right)-1\right]^{2}-1\right) -$$
$$w_{CH}\left(\left[\exp\left(-\alpha_{CH}(\rho_{CH}-\rho_{CH}^{e})\right)-1\right]^{2}-1\right) +$$
$$V_{O}\exp(-\beta_{CC}\rho_{CC}-\beta_{CH}\rho_{CH})$$
(10.56)

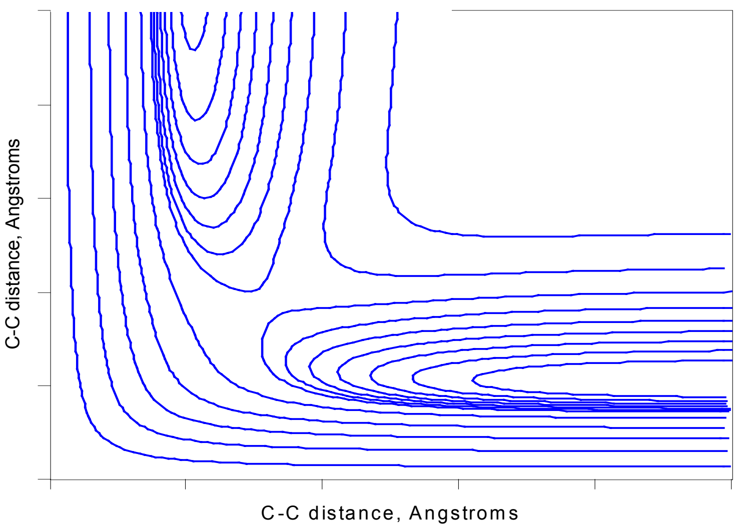

Figure 10.28 A potential energy surface calculated from equation (10.59) with w_{CC} = 95 kcal/mole, w_{CH} = 104 kcal/mole, V_P = 300 kcal/mole, q_{CC} = 0.7, q_{CH} = 0.5.

Solve for Saddle point

$$E_a = \begin{cases} 0 & \text{When } \Delta H_r / 4E_A^o < -1 \\ \dfrac{(w_O + 0.5\Delta H_r)(V_P - 2w_O + \Delta H_r)^2}{(V_P)^2 - 4(w_O)^2 + (\Delta H_r)^2} & \text{When } -1 \le \Delta H_r / 4E_A^o \le 1 \\ \Delta H_r & \text{When } \Delta H_r / 4E_A^o > 1 \end{cases}$$

(10.63)

$$w_O = (w_{CC} + w_{CH}) / 2$$

(10.64)

$$V_P = 2w_O \left(\frac{w_O + E_A^O}{w_O - E_A^O} \right)$$

(10.65)

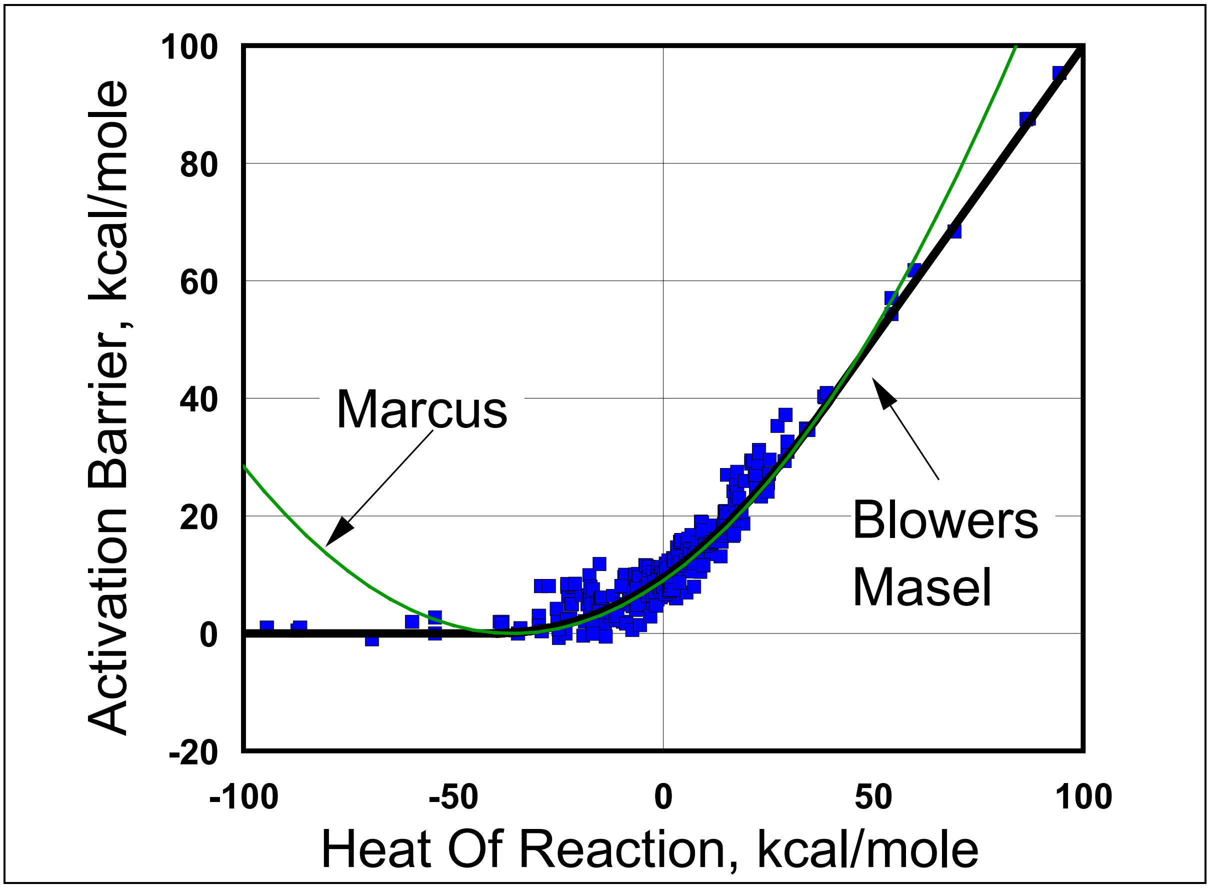

Figure 10.29 A comparison of the barriers computed from Blowers and Masel's model to barriers computed from the Marcus equation and to data for a series of reactions of the form $R + HR^1 \rightarrow RH + R^1$ with $w_O = 100$ kcal/mole and $E_A^O = 10$ kcal/mole.

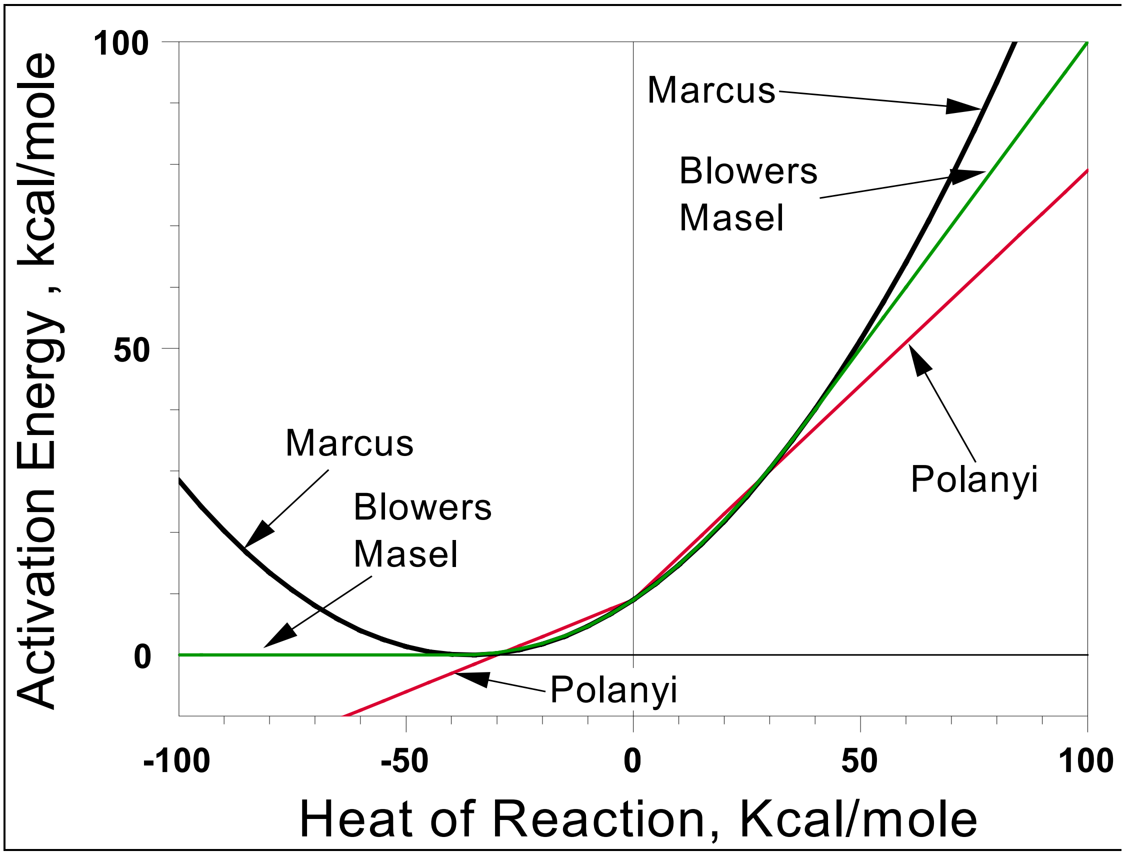

Figure 10.32 A comparison of the Marcus Equation, The Polanyi relationship and the Blowers Masel approximation for E_a^o=9 kcal/mole and w_O = 120 kcal/mole.

Table 11.3 Suggested values of the intrinsic barriers for elementary gas phase reactions. These values are used to estimate the activation barrier using the Blowers-Masel approximation.

Reaction	Intrinsic Barrier range, kcal/mole	Best estimate of the Intrinsic Barrier, kcal/mole
Atom transfer reactions (e.g $RH + X \rightarrow R + HX$)	7-15	10
Ligand transfer reactions to hydrogen (i.e. $H + R\text{-}X \rightarrow HR + X$)	40-50	45
Other ligand transfer reaction	usually 40-60	50
β – Scissions	10-20	15

Example 11.F Activation barriers via the Blowers-Masel approximation

Use a) the Blowers-Masel approximation b) the Marcus equation to estimate the activation barrier for the reaction

$H + CH_3CH_3 \rightarrow H_2 + CH_2CH_3$

Solution

a) According to the Blowers Masel approximation, the activation barrier is given by equation 11.37

$$E_a = \left(w_o + 0.5 * \Delta H_r\right)\left(\frac{\left(V_p - 2w_o + \Delta H_r\right)^2}{(V_p)^2 - 4(w_o)^2 + (\Delta H_r)^2}\right) \quad (11.F.1)$$

where w_o is the average bond energy of the bonds which break and form, ΔH_r is the heat of reaction, and V_P is given by:

$$V_P = 2w_o\left(\frac{w_o + E_A^0}{w_o - E_A^0}\right)$$

(11.F.2)

Where E_A^0 is the intrinsic barrier given in Table 11.3. According to table 11.3 E_A^0=10 kcal/mole. One could calculate a value of w_o from data in the CRC. However, I decided to assume a typical value for a C-H bond, i.e. 100 kcal/mole. I choose ΔH_r=-2 kcal/mole from example 11.C

Plugging into equation (11.F.2) shows

$$V_P = 2(100\text{kcal}/\text{mole})\left(\frac{100\text{kcal}/\text{mole} + 10\text{kcal}/\text{mole}}{100\text{kcal}/\text{mole} - 10\text{kcal}/\text{mole}}\right) = 244.4\text{kcal}/\text{mole}$$

(11.F.3)

Plugging into equation 11.F.1 shows

$$E_a = \left(100\text{kcal/mole} + 0.5 * (-2\text{kcal/mole})\right)\left(\frac{\left(244.4\text{kcal/mole} - 2(100\text{kcal/mole}) + (-2\text{kcal/mole})\right)^2}{(V_p)^2 - 4\left(w_o\right)^2 + \left(\Delta H_r\right)^2}\right) = 9.0\text{Kcal/mole}$$

By comparison the experimental value from Westley is 9.6 kcal/mole.

Limitations of the model: quantum effects:

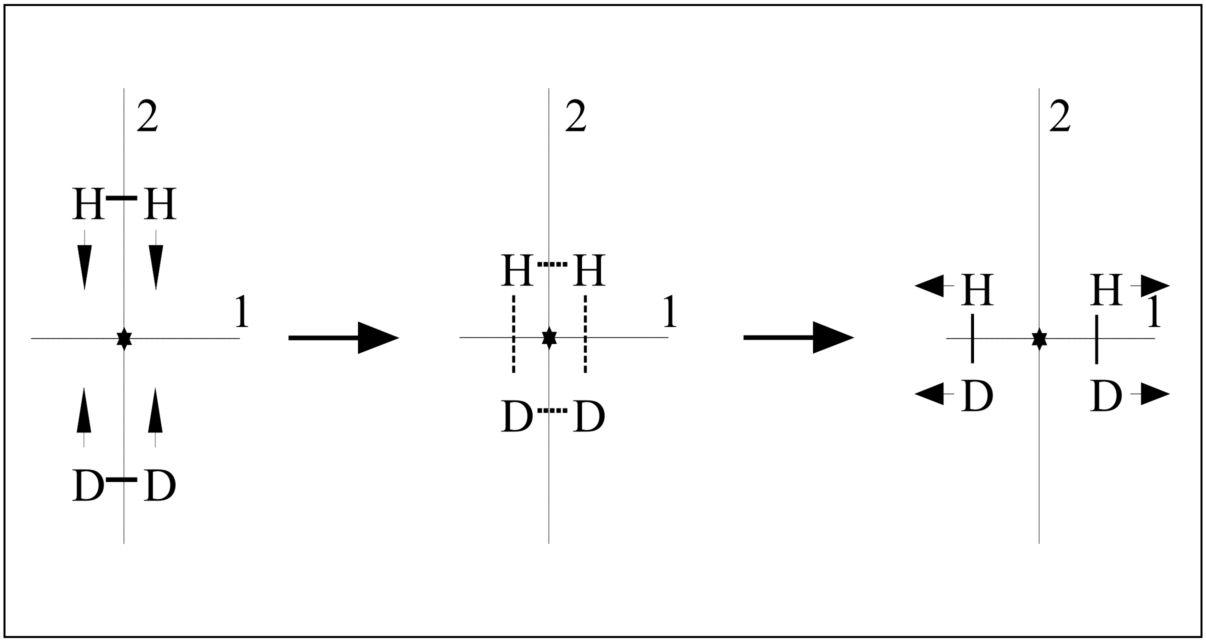

Figure 10.39 A hypothetical four-centered mechanism for H_2/D_2 exchange. The dotted lines in the figure denotes mirror planes which are preserved during the reaction (see the text). This reaction is symmetry forbidden.

Note one electron has to be spin up and spin down at the same time.

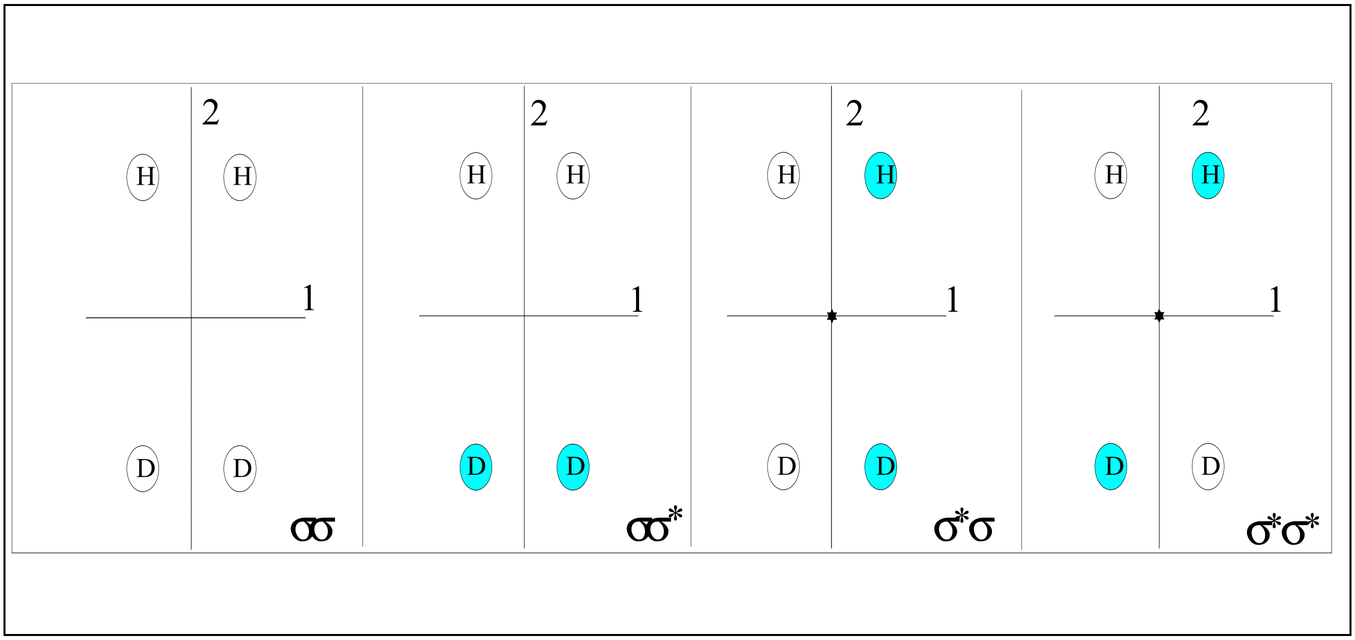

Figure 10.40 A schematic of the key molecular orbitals for the transition state of reaction (10.92). Positive atomic orbitals are depicted as open circles, negative orbitals are depicted as shaded circles.

Symmetry forbidden reactions
Woodward hoffman rules

Summary:

- Bonds need to stretch or distort during reaction. It costs energy to stretch or distort bonds. Bond stretching and distortion is one of the major causes of barriers to reaction.
- In order to get molecules close enough to react, the molecules need to overcome Pauli repulsions (i.e., electron electron repulsions) and other steric effects. The Pauli repulsions are another major cause of barriers to reaction.
- In certain special reactions, there are quantum effects which prevent the bonds in the reactants from converting smoothly from the reactants to the products. Quantum effects can produce extra barriers to reaction.
- There are also a few special cases where the reactants need to be promoted into an excited state before a reaction can occur. The excitation energy provides an additional barrier to reaction.

Polayni: linear potential
marcus: parabolic potential
Blowers-masel - size of TST varies.

Fails with quantum effects (E_A^o varies)